Received: 11 January 2022 | Revised: 19 April 2022 | Accepted: 08 May 2022

DOI: 10.1002/hep.32569

ORIGINAL ARTICLE

OPEN

# Lipocalin-2 activates hepatic stellate cells and promotes nonalcoholic steatohepatitis in high-fat diet–fed Ob/Ob mice

Kyung Eun Kim[1] | Jaewoong Lee[1] | Hyun Joo Shin[1] | Eun Ae Jeong[1] | Hye Min Jang[1] | Yu Jeong Ahn[1] | Hyeong Seok An[1] | Jong Youl Lee[1] | Meong Cheol Shin[2] | Soo Kyoung Kim[3] | Won Gi Yoo[4] | Won Ho Kim[5] | Gu Seob Roh[1]

[1]Department of Anatomy and Convergence Medical Science, College of Medicine, Institute of Health Sciences, Gyeongsang National University, Jinju, Republic of Korea

[2]College of Pharmacy, Research Institute of Pharmaceutical Sciences, Gyeongsang National University, Jinju, Republic of Korea

[3]Department of Internal Medicine, College of Medicine, Institute of Health Sciences, Gyeongsang National University, Jinju, Republic of Korea

[4]Department of Parasitology and Tropical Medicine, College of Medicine, Institute of Health Sciences, Gyeongsang National University, Jinju, Republic of Korea

[5]Division of Cardiovascular Diseases, Center for Biomedical Sciences, Korea National Institute of Health, Cheongju, Republic of Korea

**Correspondence**
Gu Seob Roh, Department of Anatomy, College of Medicine, Gyeongsang National University, 15, Jinju-daero 816 Beon-gil, Jinju-si, Gyeongnam, 52727, Republic of Korea.
Email: anaroh@gnu.ac.kr

**Funding information**
National Research Foundation of Korea, Grant/Award Number: 2015R1A5A2008833, 2018R1A6A3A01012427 and 2021R1A2C2093913.

## Abstract

**Background and Aims:** In obesity and type 2 diabetes mellitus, leptin promotes insulin resistance and contributes to the progression of NASH via activation of hepatic stellate cells (HSCs). However, the pathogenic mechanisms that trigger HSC activation in leptin-deficient obesity are still unknown. This study aimed to determine how HSC-targeting lipocalin-2 (LCN2) mediates the transition from simple steatosis to NASH.

**Approach and Results:** Male wild-type (WT) and ob/ob mice were fed a high-fat diet (HFD) for 20 weeks to establish an animal model of NASH with fibrosis. Ob/ob mice were subject to caloric restriction or recombinant leptin treatment. Double knockout (DKO) mice lacking both leptin and lcn2 were also fed an HFD for 20 weeks. In addition, HFD-fed ob/ob mice were treated with gadolinium trichloride to deplete Kupffer cells. The LX-2 human HSCs and primary HSCs from ob/ob mice were used to investigate the effects of LCN2 on HSC activation. Serum and hepatic LCN2 expression levels were prominently increased in HFD-fed ob/ob mice compared with normal diet-fed ob/ob mice or HFD-fed WT mice, and these changes were closely linked to liver fibrosis and increased hepatic α-SMA/matrix metalloproteinase 9 (MMP9)/signal transducer and activator of transcription 3 (STAT3) protein levels. HFD-fed DKO mice showed a marked reduction of α-SMA protein compared with HFD-fed ob/ob mice. In particular, the colocalization of LCN2 and α-SMA was increased in HSCs from HFD-fed ob/ob mice. In primary HSCs from ob/ob mice, exogenous LCN2 treatment induced HSC activation and

**Abbreviations:** α-SMA, α-smooth muscle actin; ACC1, acetyl-CoA carboxylase 1; ANOVA, analysis of variance; CR, caloric restriction; DEG, differentially expressed gene; DKO, double knockout; ECM, extracellular matrix; FAS, fatty acid synthase; HFD, high-fat diet; HSC, hepatic stellate cell; iNOS, inducible nitric oxide synthase; LCN2, lipocalin-2; LD, lipid droplet; LPS, lipopolysaccharide; LTM, LPS-treated medium; Ly6G, lymphocyte antigen 6 complex locus G6D; mHSC, primary mouse HSC; MMP9, matrix metalloproteinase 9; MPO, myeloperoxidase; mRNA, messenger RNA; ND, normal diet; pSTAT3, phosphorylated STAT3; rLCN2, recombinant LCN2; SCD1, stearoyl-CoA desaturase 1; siRNA, small interfering RNA; STAT3, signal transducer and activator of transcription 3; TG, triglyceride; WT, wild type.

Supplemental Digital Content is available for this article. Direct URL citations appear in the printed text and are provided in the HTML and PDF versions of this article on the journal's website, www.hepjournal.com.

MMP9 secretion. By contrast, LCN2 receptor 24p3R deficiency or a STAT3 inhibitor reduced the activation and migration of primary HSCs.

**Conclusions:** LCN2 acts as a key mediator of HSC activation in leptin-deficient obesity via α-SMA/MMP9/STAT3 signaling, thereby exacerbating NASH.

## INTRODUCTION

NAFLD, characterized by a rise in intrahepatic triglyceride (TG) content, is more common in people with obesity, insulin resistance, and type 2 diabetes.[1] NAFLD ranges from simple steatosis without hepatocellular injury to NASH, which involves steatosis, inflammation, and ballooning with or without fibrosis.[2,3] As individuals with obesity and NASH have a substantially higher risk of developing advanced hepatic fibrosis and hepatocellular carcinoma than those with simple steatosis, it is important to identify the mechanisms underlying the progression from simple steatosis to NASH.

Obesity and NAFLD increase levels of leptin, a proinflammatory adipocytokine.[4] Leptin promotes insulin resistance and contributes to the development of NASH via activation of hepatic stellate cells (HSCs).[5] HSC activation is a landmark event in leptin-mediated fibrosis because HSCs become the primary source of fibrous extracellular matrix (ECM) in NASH-related fibrosis.[6,7] Although leptin deficiency was found to cause excessive NAFLD without triggering liver fibrosis,[8] feeding a high-fat, fructose, and cholesterol diet to leptin-deficient ob/ob mice promotes liver fibrosis.[9] Thus, the role of leptin-independent signaling in NASH-related HSC activation is still unclear.

Lipocalin-2 (LCN2), a neutrophil gelatinase-associated lipocalin that transports lipophilic molecules such as lipopolysaccharide (LPS), steroids, retinoic acid, and iron, was initially purified from neutrophil granules.[10] LCN2 is a proinflammatory adipocytokine causally involved in obesity-related metabolic complications that may be considered as a prognostic biomarker of hepatic injury.[11,12] However, LCN2 appears to play paradoxical roles in the progression from steatosis to NASH.[13] Whereas one study reports that LCN2 mediates NASH by promoting neutrophil-macrophage crosstalk via the induction of chemokine (C-X-C motif) receptor 2,[13] another study shows that hepatocyte LCN2 protects against NAFLD by regulating lipolysis, lipid peroxidation, and apoptosis.[14] However, the direct role of LCN2 on the activation of HSCs in NASH-related fibrosis is not fully understood.

In the present study, we hypothesized that in high-fat diet (HFD)-fed leptin-deficient ob/ob mice, LCN2 increases hepatic α-smooth muscle actin (α-SMA)/matrix metalloproteinase 9 (MMP9)/signal transducer and activator of transcription 3 (STAT3) signaling via activation of HSCs and leads to NASH with fibrosis. In particular, we found that LCN2 promoted the migration of activated HSCs to fibrotic regions in HFD-fed ob/ob mice, and LCN2 depletion inhibited the increase in hepatic fibrosis by downregulating α-SMA/MMP9/STAT3 signaling. Thus, we revealed an association between LCN2 expression and α-SMA production in the process of HSC activation and found that LCN2 promotes NASH progression in leptin-deficient ob/ob mice through the α-SMA/MMP9/STAT3 pathway.

## MATERIALS AND METHODS

### Experimental animal models

Male wild-type (WT) C57BL/6J and leptin-deficient ob/ob mice were purchased from Central Laboratory Animal, Inc. (Seoul, South Korea). To generate LCN2-deficient ob/ob double knockout (DKO) mice, heterozygous ob/ob mice were crossed with LCN2 knockout mice (The Jackson Laboratory, Bar Harbor, ME) to obtain heterozygous $LCN2^{+/-}/ob^{+/-}$ mice, which were further bred to produce DKO mice. Mice were genotyped using polymerase chain reaction of genomic DNA isolated from tail tips obtained at 4 weeks of age (Table S1). For HFD (60 kcal %)-fed NASH mouse models, WT, ob/ob, and DKO mice of at least 5 weeks of age were fed an HFD or normal diet (ND) for 20 weeks. All mice were housed in virus-free facilities on a 12-h light/12-h dark cycle. All animal experiments were performed in accordance with the National Institutes of Health Guidelines on the Use of Laboratory Animals. The Animal Care Committee for Animal Research of Gyeongsang National University (GNU) approved the study protocol (GNU-190701-M0033).

To determine the role of LCN2 in NASH progression, male C57BL/6 mice, 3 weeks of age, were fed an ND (5% kcal from fat, Harlan Laboratories, Inc., Indianapolis, IN) or an HFD (60% kcal fat, Research Diets, New Brunswick, NJ) for 10, 20, or 30 weeks. To rule out the role of leptin in hepatic inflammation, male C57BL/6 mice received an intraperitoneal injection of 1 mg/kg $CCl_4$ (Sigma-Aldrich, St. Louis, MO) or olive oil (Sigma-Aldrich) twice a week for 4 weeks starting at 10 weeks of age. To examine whether caloric restriction (CR) reduces hepatic LCN2/α-SMA/STAT3 signaling, male ob/ob mice were transferred to individual cages and received a restricted amount of food (2 g/day) for 12 weeks after 10 weeks of free access to

food as previously described.[1] Conversely, to examine whether exogenous LCN2 increases hepatic LCN2/α-SMA/STAT3 signaling, male WT and ob/ob mice were injected intraperitoneally with recombinant LCN2 (rLCN2; 2.2 mg/mL) for 3 days prior to sacrifice at 22 weeks of age. To deplete Kupffer cells, HFD-fed ob/ob male mice were injected intraperitoneally with gadolinium trichloride ($GdCl_3$; 20 mg/kg, Sigma-Aldrich) twice a week for 10 weeks starting at 6 weeks of age. To examine the potential role of exogenous leptin in hepatic LCN2/α-SMA/STAT3 signaling in ob/ob and DKO mice, recombinant leptin (2 mg/kg) was injected intraperitoneally twice a week for 4 weeks starting at 10 weeks of age.

## Statistical analysis

Statistical analyses were performed using PRISM 7.0 (GraphPad Software Inc., San Diego, CA). Group differences were determined using unpaired Student *t* test or one-way and two-way analysis of variance (ANOVA) followed by Tukey's post hoc tests. Correlations between liver LCN2 and α-SMA and hydroxyproline levels were determined nonparametric Spearman's analysis. All values are expressed as mean ± SEM. A $p$ value <0.05 was considered statistically significant.

Further detailed information about materials and methods are provided in the supporting files.

# RESULTS

## Elevated LCN2 protein level is associated with leptin-independent NASH

Across 30 weeks of HFD feeding, HFD-fed WT mice exhibited increased metabolic parameters and NAFLD activity scores compared with ND-fed WT mice (Figure S1A–G). There was a considerable increase in hepatic α-SMA protein after 20 weeks of HFD feeding (Figure 1H). Notably, although the increase in serum leptin was sustained after 10 weeks of HFD feeding, serum LCN2 and its liver messenger RNA (mRNA) and protein levels increased in a time-dependent manner after 20 weeks of HFD feeding (Figure 1I–L).

To determine the role of leptin and LCN2 in animal mouse models of liver injury, we used nutritional HFD-fed, genetic ob/ob, and chemical $CCl_4$-treated mice (Figure 1). Whereas both HFD-fed and ob/ob mice had fatty liver and higher hepatic TG levels than ND-fed and $CCl_4$-treated mice, $CCl_4$-treated mice exhibited the most pronounced fibrotic changes (Figure 1A–C). Notably, although ob/ob and $CCl_4$-treated mice had lower serum leptin levels than HFD-fed mice, they had higher circulating and liver protein levels of LCN2 that were closely linked to Sirius Red–stained fibrotic changes and higher numbers of LCN2-positive cells and F4/80-positive macrophages (Figure 1D–H). Taken together, these findings suggest that elevated LCN2 may be closely associated with NASH without increased leptin levels.

## Higher circulating and hepatic LCN2 levels in HFD-fed OB/OB mice with elevated hepatic α-SMA protein and fibrotic changes

To rule out leptin-dependent liver fibrosis, leptin-deficient ob/ob mice were fed an HFD for 20 weeks. As expected, HFD-fed ob/ob mice had higher body weights and fat mass, increased total cholesterol, and greater insulin resistance than ob/ob or HFD-fed WT mice (Figure S2). Compared with ND-fed WT mice, HFD-fed WT mice and HFD- or ND-fed ob/ob mice showed typical NAFLD characterized by accumulation of hepatic TG, increased liver weight and hepatic enzyme levels, and a higher NAFLD activity score (Figure 2A–G). Notably, circulating LCN2, as well as its liver mRNA and protein levels, were increased in HFD-fed ob/ob mice and were accompanied by larger Sirius Red–stained fibrotic areas and higher hepatic α-SMA protein levels (Figure 2H–L). Interestingly, liver LCN2 protein levels were positively associated with α-SMA expression and hydroxyproline levels in HFD-fed ob/ob mice (Figure S3A–C). Furthermore, double immunofluorescence revealed that many TGF-β1–positive cells colocalized with collagen 1–positive cells in HFD-fed ob/ob mice (Figure S3D). These findings suggest that LCN2-related signaling may play a key role in α-SMA–mediated fibrosis in NASH mice with leptin deficiency.

## Elevated LCN2 is associated with increased hepatic MMP9 and STAT3 expression in HFD-fed OB/OB mice

To gain further insight into the role of LCN2 in NASH progression with leptin loss, we performed RNA sequencing–based transcriptome analysis of WT and ob/ob mice fed an HFD or ND. Two-way ANOVA with genotype and HFD factors identified statistically significant changes in 6280 genes ($p < 0.05$). In unbiased hierarchical clustering and principal components analysis, all groups clustered clearly, with a separation between ob/ob and WT groups along principal component 1 accounting for 54.2% of the variation among groups (Figure 3A,B). The relative position of the groups demonstrates that the effect of HFD can be examined using the most significantly upregulated genes in both HFD-fed WT and ob/ob mice. We identified a total of 1111 differentially expressed genes (DEGs), with significant upregulation of 814 and 64 genes in WT and ob/ob mice, respectively, with a $\log_2FC \geq 1.0$ and adjusted $p < 0.05$ (Figure 3C). Of these, eight HFD-upregulated

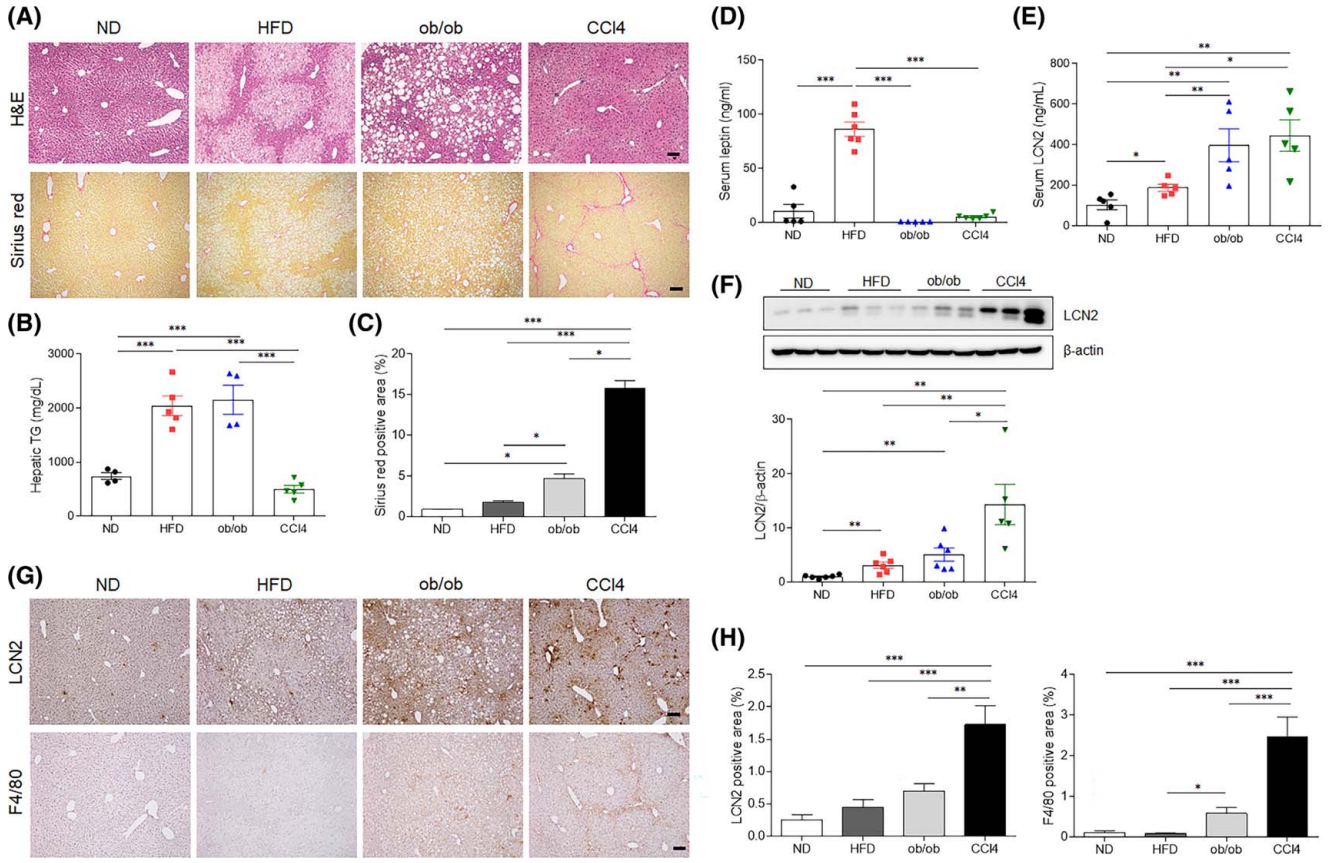


**FIGURE 1** Lipocalin-2 (LCN2) expression is upregulated in liver injury. (A) Representative hematoxylin and eosin (H&E) and Sirius Red staining of liver sections. Scale bars, 100 μm. (B) Hepatic triglyceride (TG; $n = 4–5$). (C) Sirius Red–positive area. (D,E) Serum leptin and LCN2 levels ($n = 5–6$). (F) Western blot analysis and quantification of LCN2 protein ($n = 5–6$). (G) Representative LCN2 and F4/80 staining of liver sections. Scale bars, 100 μm. (H) Quantification of LCN2- and F4/80-positive areas. Significance was determined by one-way analysis of variance. HFD, high-fat diet; ND, normal diet. $^*p < 0.05$, $^{**}p < 0.01$, $^{***}p < 0.001$.

genes were chosen as key regulatory genes in both WT and ob/ob mice (Figure 3D, Table S2). *Lcn2*, *Circadian-associated transcriptional repressor*, and *Cytochrome P450 3a57* were significantly expressed in both HFD and ob/ob conditions, but, as expected, *Lcn2* expression was upregulated in both HFD-fed strains of mice ($\log_2$FC = 5.90 and 1.87 for WT and ob/ob, respectively, $p < 0.05$). Using the STRING database,[15] we determined that LCN2 interacts with MMP9 as evidenced by comigration in nondenaturing gel electrophoresis with an interaction score of 0.40 (Figure 3E) and significantly comentioned proteins in the literature with an interaction score of 0.99.[16] In functional enrichment analysis, we identified dysregulated gene sets including both *Lcn2* and *Mmp9* that are involved in inflammatory obesity, including granulocyte, IL-17 signaling pathway, and cellular response to reactive oxygen species (Figure 3F).

LCN2 forms a heterodimer with MMP9, with the interaction between LCN2 and MMP9 enhancing MMP9 activation.[17] In line with LCN2 expression levels, HFD-fed ob/ob mice had higher MMP9 protein levels than ND-fed ob/ob mice (Figure 4A). Zymography and immunoprecipitation analyses showed that HFD-fed ob/ob mice had higher levels of hepatic LCN2/MMP9 complex than HFD-fed WT or ND-fed ob/ob mice (Figure 4B and 4C). Furthermore, Duolink assay showed the presence of many LCN2/MMP9-positive cells within and around portal triad lesions in HFD-fed ob/ob mice (Figure 4D). LCN2 and MMP9 are controlled by the transcription factor STAT3.[18,19] Thus, as expected, HFD-fed ob/ob mice showed significant upregulation of phosphorylated STAT3 (pSTAT3)/STAT3 expression (Figure 4E).

To examine whether LCN2 plays a role in MMP9 and pSTAT3 upregulation, we examined the effects of CR on LCN2/MMP9/STAT3 signaling in ob/ob mice (Figure S4A). Consistent with our previous study showing that CR attenuates circulating LCN2 levels in ob/ob mice,[20] we found that CR significantly attenuated the increased hepatic LCN2/MMP9/pSTAT3 protein expression in ob/ob mice (Figure S4B–D). By contrast, rLCN2 treatment increased hepatic LCN2/MMP9/pSTAT3 protein expression in ob/ob mice (Figure S5). These findings suggest that LCN2-mediated MMP9/STAT3 signaling may play an important role in the pathogenesis of NASH.

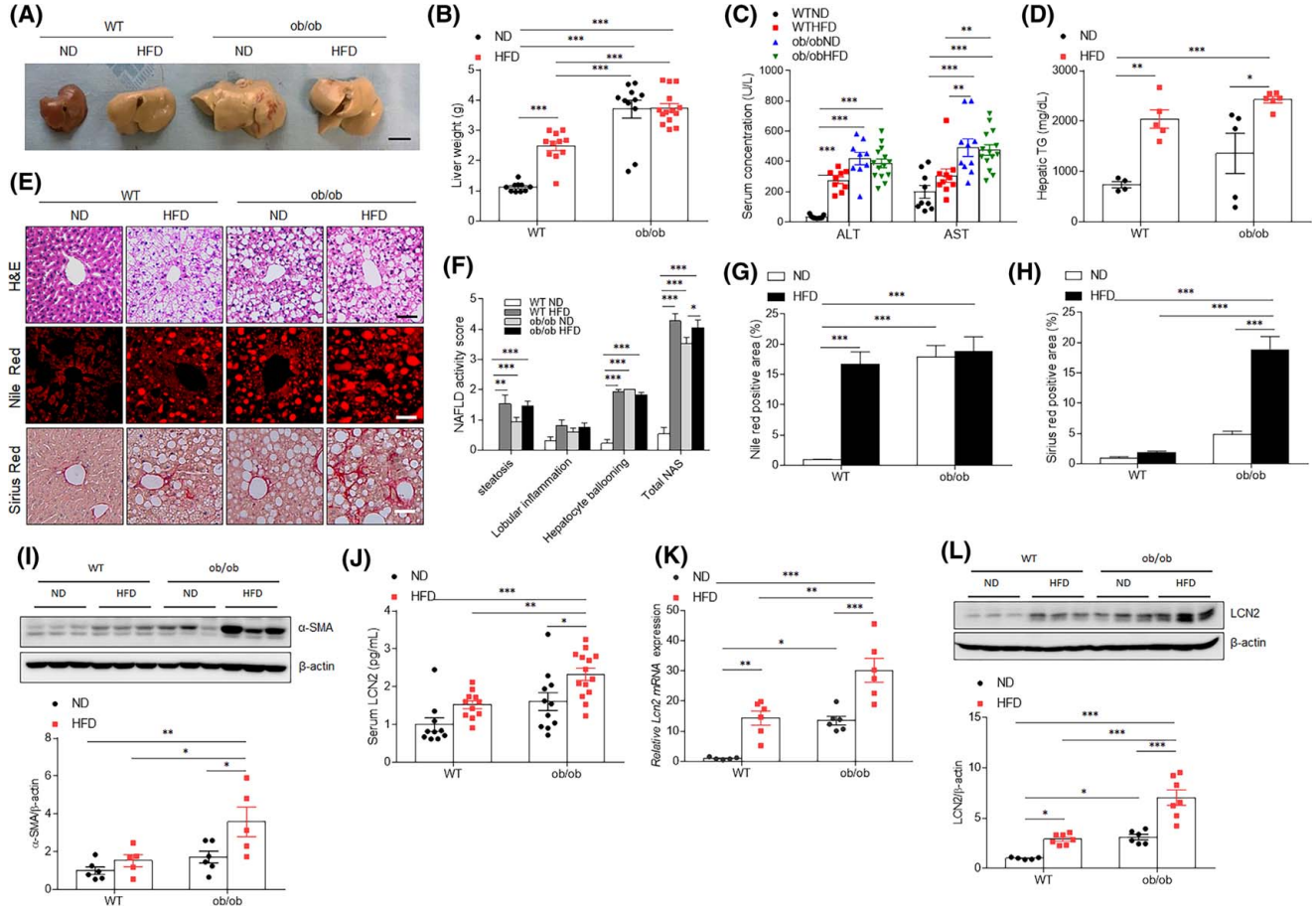


**FIGURE 2** Increased hepatic fibrosis is linked to increased lipocalin-2 (LCN2) levels in high-fat diet (HFD)-fed Ob/Ob mice. Wild-type (WT) and Ob/Ob mice were fed a normal diet (ND) or HFD for 20 weeks to induce NASH with fibrosis. (A) Representative images of livers from mice after 20 weeks of ND or HFD feeding. Scale bars, 1 cm. (B–D) Liver weight ($n$ = 10–14), serum alanine aminotransferase (ALT) and aspartate aminotransferase (AST) ($n$ = 9–10), and hepatic triglycerides (TG; $n$ = 4–7). (E) Representative hematoxylin and eosin (H&E), Nile Red, and Sirius Red staining of liver tissue. Scale bars, 50 μm. (F–H) NAFLD activity score (NAS), Nile Red–positive area, and Sirius Red–positive area. (I) Western blot analysis and quantification of α-smooth muscle actin (α-SMA) protein in liver lysates ($n$ = 5–6). (J–L) Serum LCN2 ($n$ = 10–14), hepatic LCN2 messenger RNA, and protein levels ($n$ = 5–7). Significance was determined by two-way analysis of variance. $^*p < 0.05$, $^{**}p < 0.01$, $^{***}p < 0.001$. ob/obHFD, HFD-fed ob/ob; ob/obND, ND-fed ob/ob; WTHFD, HFD-fed WT; WTND, ND-fed WT.

## Exogenous leptin does not affect hepatic α-SMA expression in mice lacking both leptin and LCN2

Given that exogenous leptin could induce hepatic α-SMA/MMP9/STAT3 expression, recombinant leptin (2 mg/kg) was intraperitoneally injected two times weekly for 4 weeks in ob/ob or DKO mice (Figure S6A–C). Serum leptin was measurable in both groups, but LCN2 was absent in DKO mice (Figure S6D,E). Except for fat mass and serum aspartate aminotransferase, which was significantly reduced in DKO mice compared with ob/ob mice after leptin treatment, we saw no other changes in metabolic parameters (Figure S6F–L). Although leptin treatment slightly increased MMP9/STAT3 expression in DKO mice compared with ob/ob mice, there was no increase in α-SMA in leptin-treated DKO mice (Figure S6M,N). Furthermore, histological analysis showed no difference in lipid droplets (LDs) or fibrotic areas in leptin-treated ob/ob or DKO mice (Figure S6O,P). These results indicate that leptin does not promote hepatic α-SMA–related fibrosis through MMP9/STAT3 signaling in LCN2-deficient ob/ob mice.

## LCN2 deletion attenuates hepatic α-SMA expression in HFD-fed OB/OB mice by downregulating MMP9/STAT3

Given that LCN2 and MMP9 are regulated by STAT3, which is a major downstream effector of IL-6,[19] and that chronic hepatic inflammation and repair cause excessive accumulation of ECM, which regulates turnover in hepatic fibrosis via MMPs,[21] we hypothesized that genetic depletion of LCN2 could reduce hepatic α-SMA/MMP9/STAT3 and NF-kBp65 signaling in HFD-fed ob/ob mice. First, we found that Duolink assay reveals LCN2 loss in DKO mice. Duolink signals, indicating LCN2 and its receptor 24p3R interaction or close distance, were more abundant in the liver sections of HFD-fed ob/ob mice

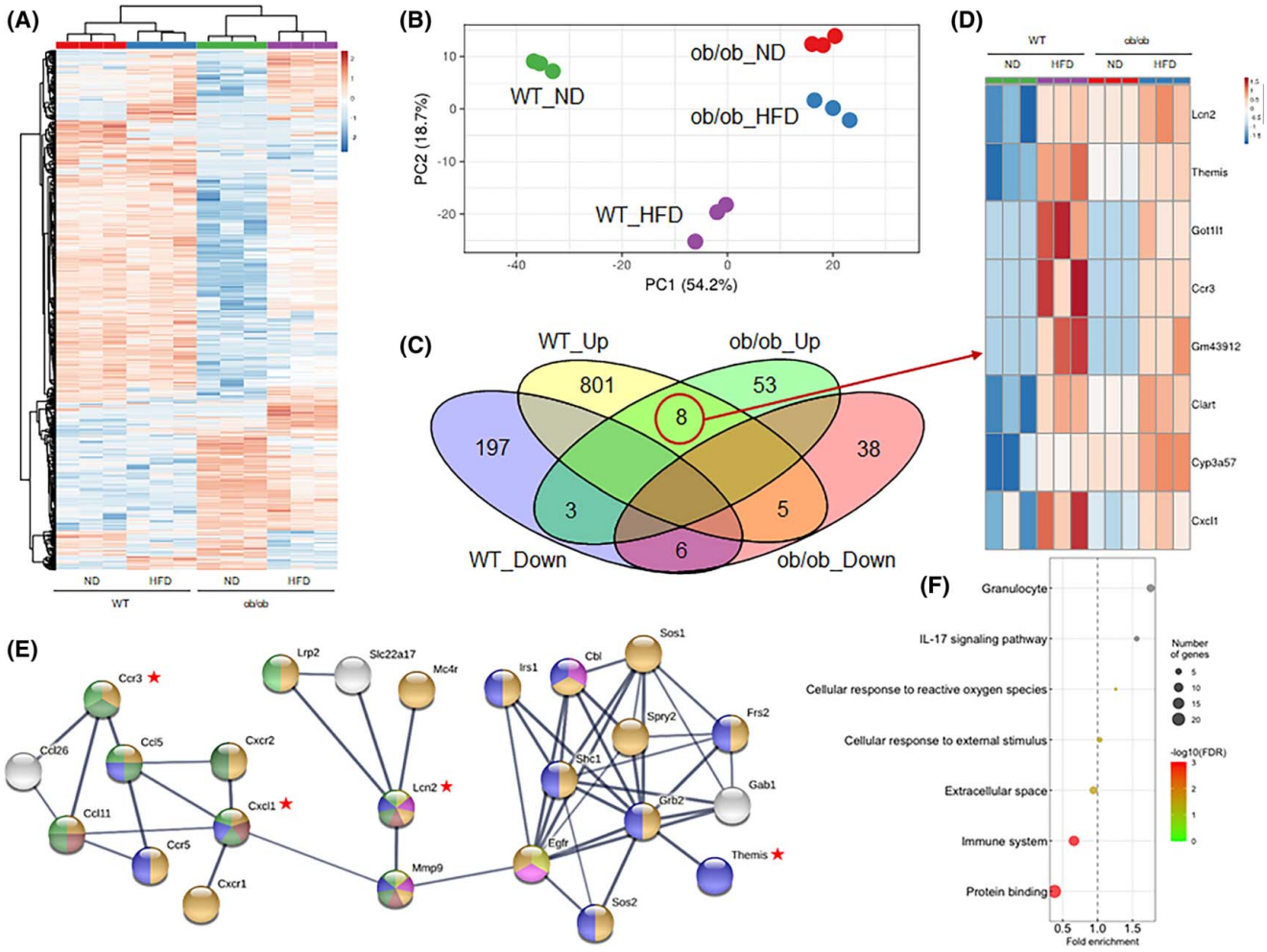


**FIGURE 3** A high-fat diet (HFD) upregulates lipocalin-2 (*Lcn2*) gene expression in mouse livers as revealed by transcriptomic profiling. Groups of wild-type (WT) or Ob/Ob mice fed a normal diet (ND) or high-fat diet (HFD; $n = 3$ per group) were discriminated clearly based on significant changes in the expression of 6280 genes in the liver ($p < 0.05$) as indicated by two-way analysis of variance using unsupervised analysis. (A) Hierarchical clustering and (B) principal components analysis. Dendrograms were generated based on hierarchical clustering of correlation distance between individual RNA-sequencing expression profiles. (C) Venn diagram showing differentially expressed genes (DEGs) in the liver affected by an HFD ($\log_2$FC $\geq 1$, adjusted $p < 0.05$). (D) Eight HFD-induced DEGs upregulated in both WT and Ob/Ob mice were considered key regulatory genes, among which *Lcn2* was the most highly expressed gene on average. (E) Protein–protein interactions of eight DEG products were constructed with no more than 10 interactors using the STRING database. Three clusters were found based on a Markov clustering algorithm, and both *Lcn2* and matrix metalloproteinase 9 (*Mmp9*) were implicated as hub genes in the regulation of each subnetwork. (F) Functional enrichment plot of both *Lcn2* and *Mmp9* showing seven gene sets (false discovery rate $< 0.05$). Cbl, Casitas B-lineage lymphoma; Ccl5, Chemokine (C-C motif) ligand 5; Ccr, Chemokine (C-C motif) receptor; Ciart, Circadian associated repressor of transcription; Cxcl, Chemokine (C-X-C motif) ligand; Cxcr, CXC chemokine receptor; Egfr, Epidermal growth factor receptor; FDR, False Discovery Rate; Frs, FAR1 related sequences; Gab, GRB2 associated binding protein; Gm43912, predicted gene 43912; Got1l1, glutamic-oxaloacetic transaminase 1-like 1; Grb, Growth factor receptor bound protein; Irs, Insulin receptor substrate; Lrp, Leucine-responsive transcriptional regulator; PCs, principal components; Shc, SHC-adaptor protein; Slc, Solute carrier; Sos, SOS Ras/Rac guanine nucleotide exchange factor; Spry, Sprouty; Themis, Thymocyte selection associated.

compared to those of HFD-fed DKO mice (Figure S7). This LCN2 depletion significantly reduced hepatic MMP9 protein levels, pSTAT3/STAT3 ratio, and serum MMP9 levels in HFD-fed ob/ob mice (Figure 5A,B). In line with Sirius Red staining (Figure 5C), LCN2 depletion markedly attenuated hepatic α-SMA mRNA and protein levels in HFD-fed ob/ob mice (Figure 5D,E).

Activation of NF-kB, which controls the transcription of various proinflammatory genes, can be assessed by nuclear translocation of its p65 subunit.[22] We found that LCN2 depletion decreased the nuclear-to-cytosolic ratio of NF-kBp65 in HFD-fed ob/ob mice (Figure 5F). Immunohistochemical analysis showed that the presence of myeloperoxidase (MPO)-positive neutrophils in liver sections from HFD-fed ob/ob mice was reduced by LCN2 depletion (Figure S8A). Translocated NF-kBp65 binds to the inducible nitric oxide synthase (iNOS) promoter and induces iNOS expression,[23] and a previous study reports that inhibition of iNOS in HSCs may have antifibrotic effects.[24] Consistent with these previous findings, DKO mice also had reduced hepatic iNOS mRNA and

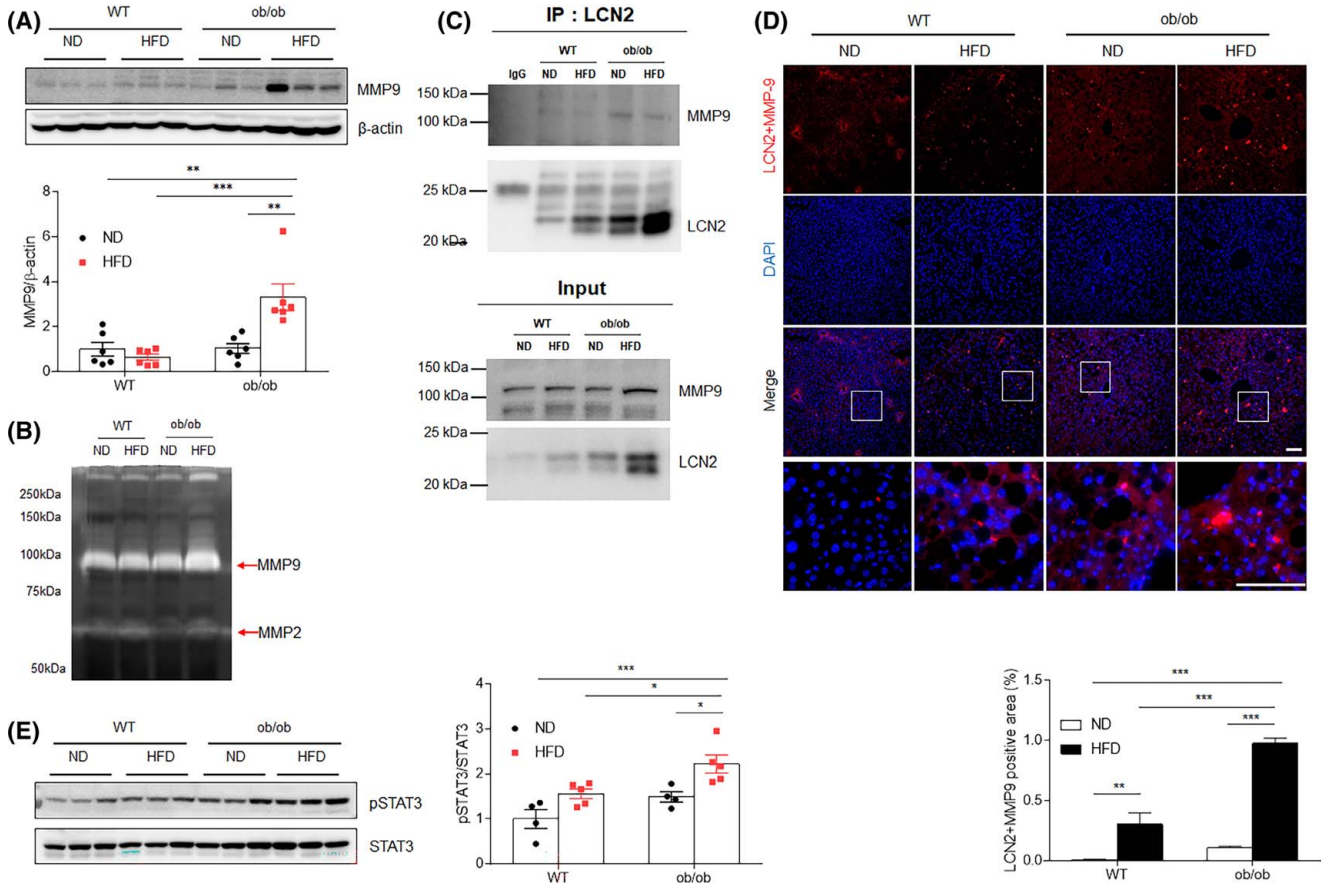


**FIGURE 4** Lipocalin-2 (LCN2) regulates hepatic fibrosis in high-fat diet (HFD)-fed Ob/Ob mice by interacting with matrix metalloproteinase 9 (MMP9). Wild-type (WT) and Ob/Ob mice were fed a normal diet (ND) or HFD for 20 weeks to induce NASH. (A) Western blot analysis and quantification of MMP9 protein in liver lysates ($n = 6$). (B) Photographs of zymography. Bands corresponding to MMP9 and MMP2 are indicated by arrows. (C) Immunoprecipitation of LCN2 and MMP9 in liver lysates. (D) Representative Duolink PLA staining of LCN2 and MMP9 in liver sections. Nuclei were stained with DAPI. Scale bar, 50 μm. Quantification of the LCN2+MMP9–positive area. (E) Western blot analysis and quantification of phosphorylated signal transducer and activator of transcription 3 (pSTAT3)/signal transducer and activator of transcription 3 (STAT3) protein in liver lysates ($n = 4$–5). Significance was determined by two-way analysis of variance. *$p < 0.05$, **$p < 0.01$, ***$p < 0.001$. DAPI, 4′,6-diamidino-2-phenylindole; IP, immunoprecipitation.

protein levels (Figure S8B,C). These findings indicate that LCN2 depletion attenuates the MMP9/STAT3 signaling pathway and prevents NASH progression in HFD-fed ob/ob mice.

## Elevated LCN2 is targeted to HSCs on NASH progression in HFD-Fed OB/OB mice

Many studies report that LCN2 plays roles in neutrophils, Kupffer cells, and hepatocytes.[11] To determine which target cells promote LCN2-mediated NASH progression in HFD-fed ob/ob mice, we performed double immunofluorescence (Figure S9). In HFD-fed ob/ob mice, many LCN2-positive cells colocalized with α-SMA–positive HSCs around the portal triad areas of fibrosis, including CD68-positive Kupffer cells and lymphocyte antigen 6 complex locus G6D (Ly6G)- and MPO-positive neutrophils (Figure S9A–D). Despite studies showing that LCN2 is linked to neutrophils and macrophages, we found that HFD-fed ob/ob mice had higher levels of LCN2 colocalization with α-SMA than CD68, Ly6G, or MPO-positive cells (Figure S9E–H). Furthermore, although $GdCl_3$-induced depletion of hepatic macrophages significantly reduced liver weight, hepatic enzymes, and F4/80 expression in HFD-fed ob/ob mice, it did not significantly affect serum LCN2, hepatic LCN2, or pSTAT3/STAT3 levels (Figure S10). These findings strongly suggest that LCN2 may promote NASH progression by targeting HSCs in HFD-fed mice with leptin deficiency.

## Elevated LCN2 promotes HSC activation in HFD-fed OB/OB mice

HSCs are filled with cytoplasmic LDs containing retinoid in the normal liver.[25,26] HSC activation is characterized by the progressive loss of LDs as HSCs transition from a quiescent to a more fibrogenic

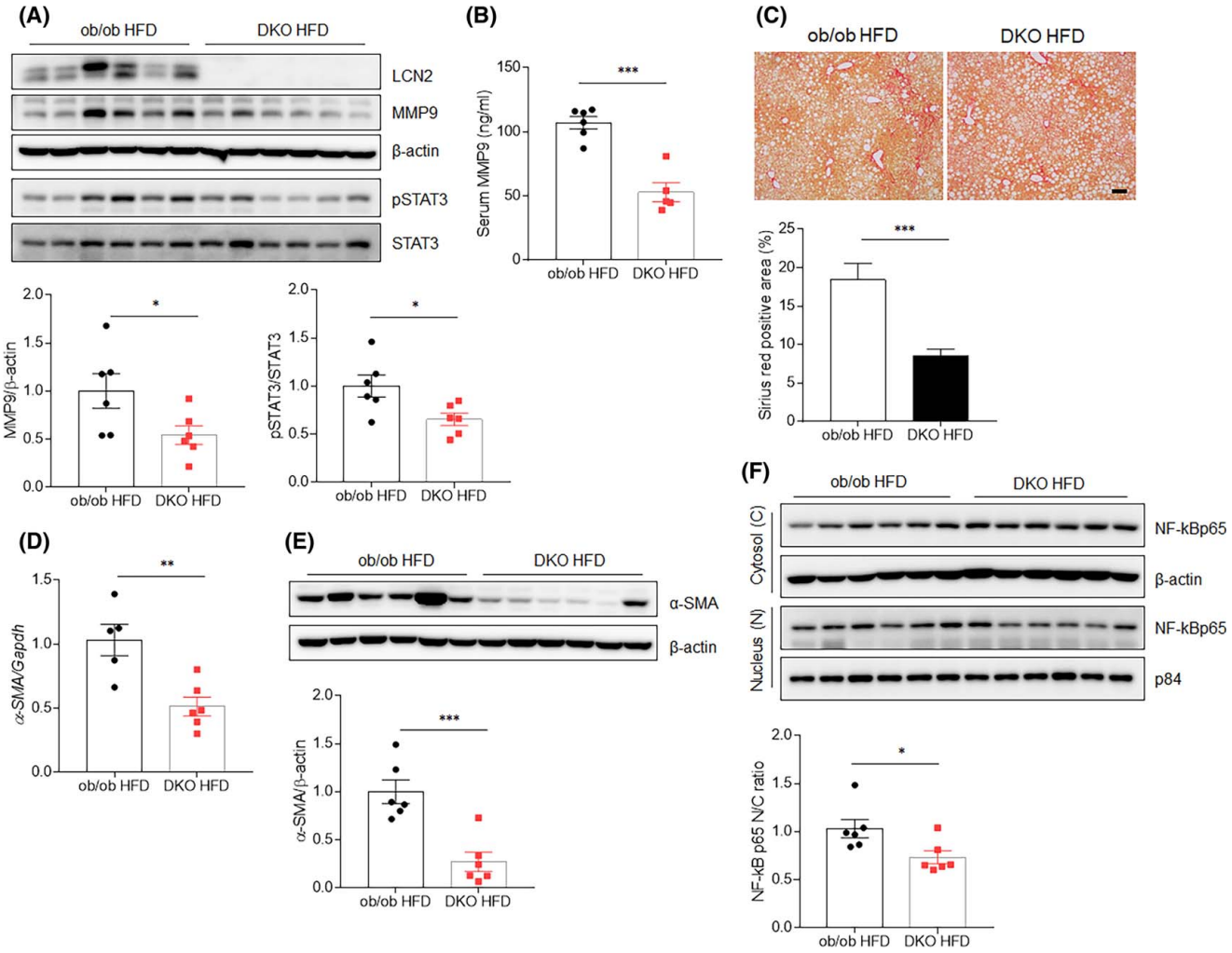


**FIGURE 5** Lipocalin-2 (LCN2) deficiency protects against high-fat diet (HFD)-induced liver fibrosis in Ob/Ob mice. Ob/Ob and double knockout (DKO) mice were fed an HFD for 20 weeks to induce NASH with fibrosis. (A) Western blot analysis and quantification of LCN2, matrix metalloproteinase 9 (MMP9), and phosphorylated signal transducer and activator of transcription 3 (pSTAT3) protein in liver lysates ($n = 5–6$). (B) Serum MMP9 was assessed by enzyme-linked immunosorbent assay ($n = 5–6$). (C) Representative images and quantification of Sirius Red staining in liver sections. Scale bars, 100 μm. (D) Hepatic α-smooth muscle actin (α-SMA) messenger RNA was measured by real-time polymerase chain reaction ($n = 5–6$). (E) Western blot analysis and quantification of α-SMA protein in liver lysates from HFD-fed Ob/Ob and DKO mice ($n = 6$). (F) Western blot analysis of cytosolic and nuclear NF-κBp65 protein and the nuclear/cytosolic (N/C) ratio of NF-κBp65 in liver lysates ($n = 6$). β-Actin and p84 were used as loading controls for total and nuclear proteins, respectively. Significance was determined by a two-tailed *t* test. $^*p < 0.05$, $^{**}p < 0.01$, $^{***}p < 0.001$. STAT3, signal transducer and activator of transcription 3.

state.[27] Cytoplasmic LDs in the liver of humans and mice are enriched in perilipin 2.[28] Together with an increase in α-SMA in HFD-fed ob/ob mice (Figure 2I), double immunofluorescence revealed that α-SMA–positive HSCs did not colocalize with perilipin 2–positive cells around portal areas in HFD-fed ob/ob mice (Figure 6A). Liver perilipin 2 protein was reduced in HFD-fed ob/ob mice compared with HFD-fed WT or ND-fed ob/ob mice (Figure 6B). After isolating primary hepatocytes, Kupffer cells, and HSCs from the livers of ob/ob mice fed an ND or HFD, we found more LCN2 proteins in all cell types in HFD-fed ob/ob mice compared with ND-fed ob/ob mice (Figure 6C). Notably, perilipin 2 and α-SMA in both hepatocytes and HSCs were decreased and increased in HFD-fed ob/ob mice, respectively (Figure 6C). Furthermore, LCN2 depletion significantly increased perilipin 2 in the liver of HFD-fed ob/ob mice (Figure 6D). HSCs isolated form HFD-fed DKO mice showed higher levels of perilipin-2 and lower levels of α-SMA than those from HFD-fed ob/ob mice (Figure 6E). Increased hepatic de novo lipogenesis-related proteins [including acetyl-CoA carboxylase 1 (ACC1), stearoyl-CoA desaturase 1 (SCD1), and fatty acid synthase (FAS)] in ND-fed ob/ob mice were significantly reduced by HFD feeding (Figure 6F). Taken together, these findings suggest that LCN2 may play a critical role in NASH with fibrosis through the progressive loss of LDs during HSC activation.

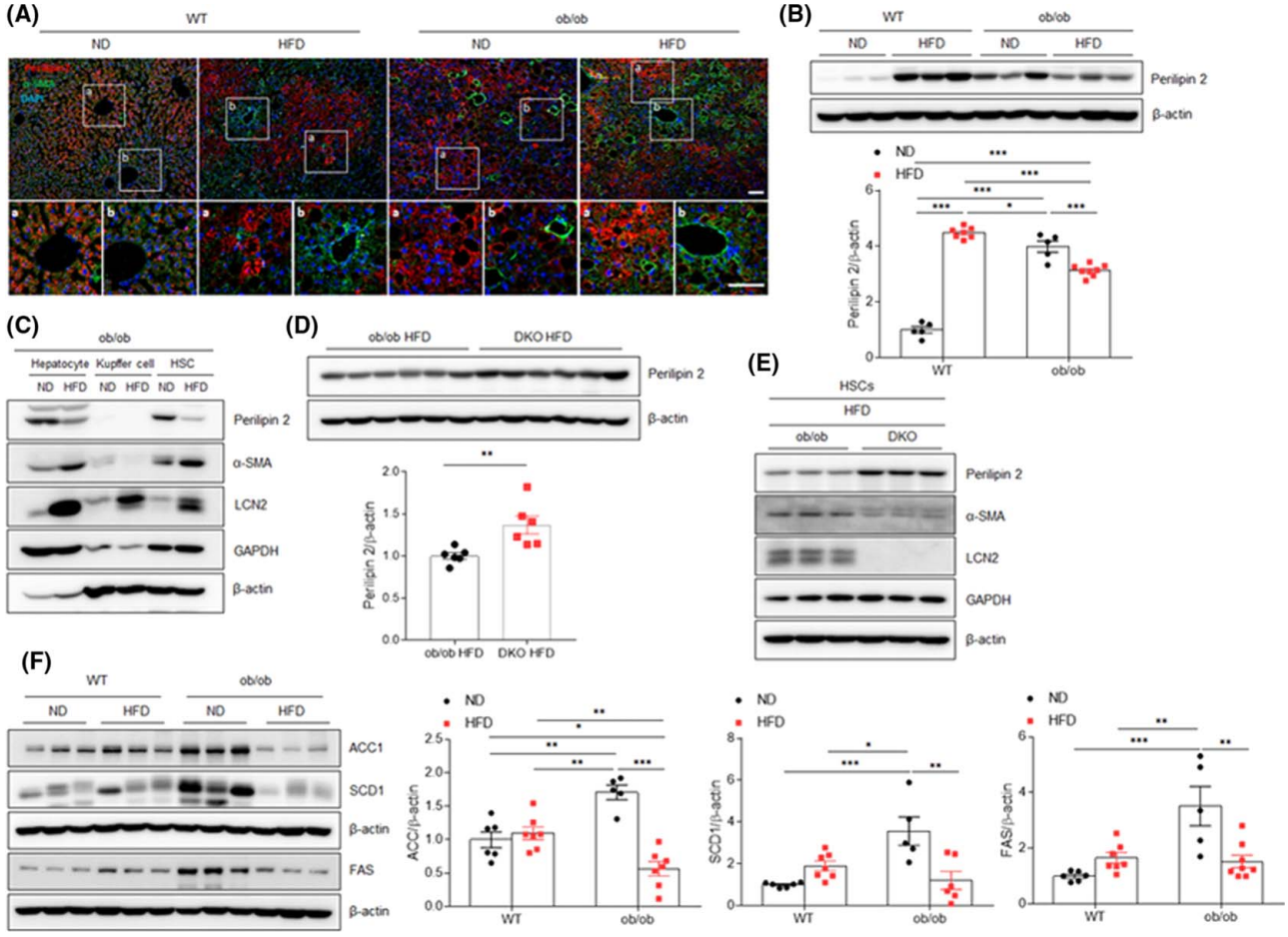


**FIGURE 6** Effects of a high-fat diet (HFD) on perilipin 2 expression in the liver of Ob/Ob mice. (A) Representative images of immunofluorescence staining of perilipin 2 and α-smooth muscle actin (α-SMA) in liver sections. Nuclei were counterstained with 4',6-diamidino-2-phenylindole (DAPI). Scale bar, 50 μm. (B) Western blot analysis and quantification of hepatic perilipin 2 protein in wild-type (WT) and Ob/Ob mice fed a normal diet (ND) or HFD ($n = 5–8$). (C) Western blot analysis of perilipin 2, α-SMA, and lipocalin-2 (LCN2) protein in hepatocytes, Kupffer cells, and hepatic stellate cells (HSCs) purified from livers of Ob/Ob mice fed an ND or HFD. (D) Western blot analysis and quantification of hepatic perilipin 2 protein in HFD-fed Ob/Ob or double knockout (DKO) mice ($n = 6$). (E) Western blot analysis of perilipin 2, α-SMA, and LCN2 protein in HSCs purified from livers of HFD-fed Ob/Ob or DKO mice ($n = 3$). (F) Western blot analysis and quantification of acetyl-CoA carboxylase 1 (ACC1), stearoyl-CoA desaturase 1 (SCD1), and fatty acid synthase (FAS) protein in liver lysates ($n = 5–8$). For (B) and (F), significance was determined by two-way analysis of variance. For (D), significance was determined by a two-tailed *t* test. GAPDH, glyceraldehyde 3-phosphate dehydrogenase. $^*p < 0.05$, $^{**}p < 0.01$, $^{***}p < 0.001$.

## Secreted LCN2 promotes HSC activation through α-SMA/MMP9/STAT3-mediated signaling

We next verified whether secreted LCN2 directly activates HSCs using human HSCs (LX-2). LPS-treated RAW 264.7 macrophages showed elevated levels of LCN2 in a time-dependent manner, and LPS-treated medium (LTM) increased the production of LCN2, TNF-α, and IL-6 proteins (Figure S11A,B). To determine the role of secreted LCN2 in the activation of HSCs, we treated LX-2 cells with LTM (Figure S11C) and found that LTM increased α-SMA levels and MMP9 release in a time-dependent manner (Figure S11D,E). In addition, we confirmed that rLCN2 increased α-SMA, pSTAT3, and MMP9 levels in LX-2 cells (Figure S11F).

We further evaluated whether LTM could induce activation of primary mouse HSCs (mHSCs) from ob/ob mice. LTM-induced mHSCs showed increased *Lcn2* and *collagen 1α* mRNA levels 12 h after treatment (Figure 7A), and LTM-induced mHSCs exhibited increased LCN2, 24p3R, α-SMA, and pSTAT3/STAT3 protein 12 h after LTM treatment as well as increased MMP9 and LCN2 secretion after 6 h in media (Figure 7B). Furthermore, we confirmed that rLCN2 increased LCN2, α-SMA, and pSTAT3 levels in mHSCs and elevated MMP9 and LCN2 secretion (Figure 7C). Inhibition of pSTAT3 by S31-101, a STAT3 inhibitor, reduced levels of LCN2, pSTAT3, and α-SMA. Also, S31-101 attenuated MMP9 and LCN2 secretion in rLCN2-treated mHSCs (Figure 7D). Taken together, these results indicate that LCN2 directly regulates activation of HSCs through STAT3-mediated signaling and MMP9 secretion.

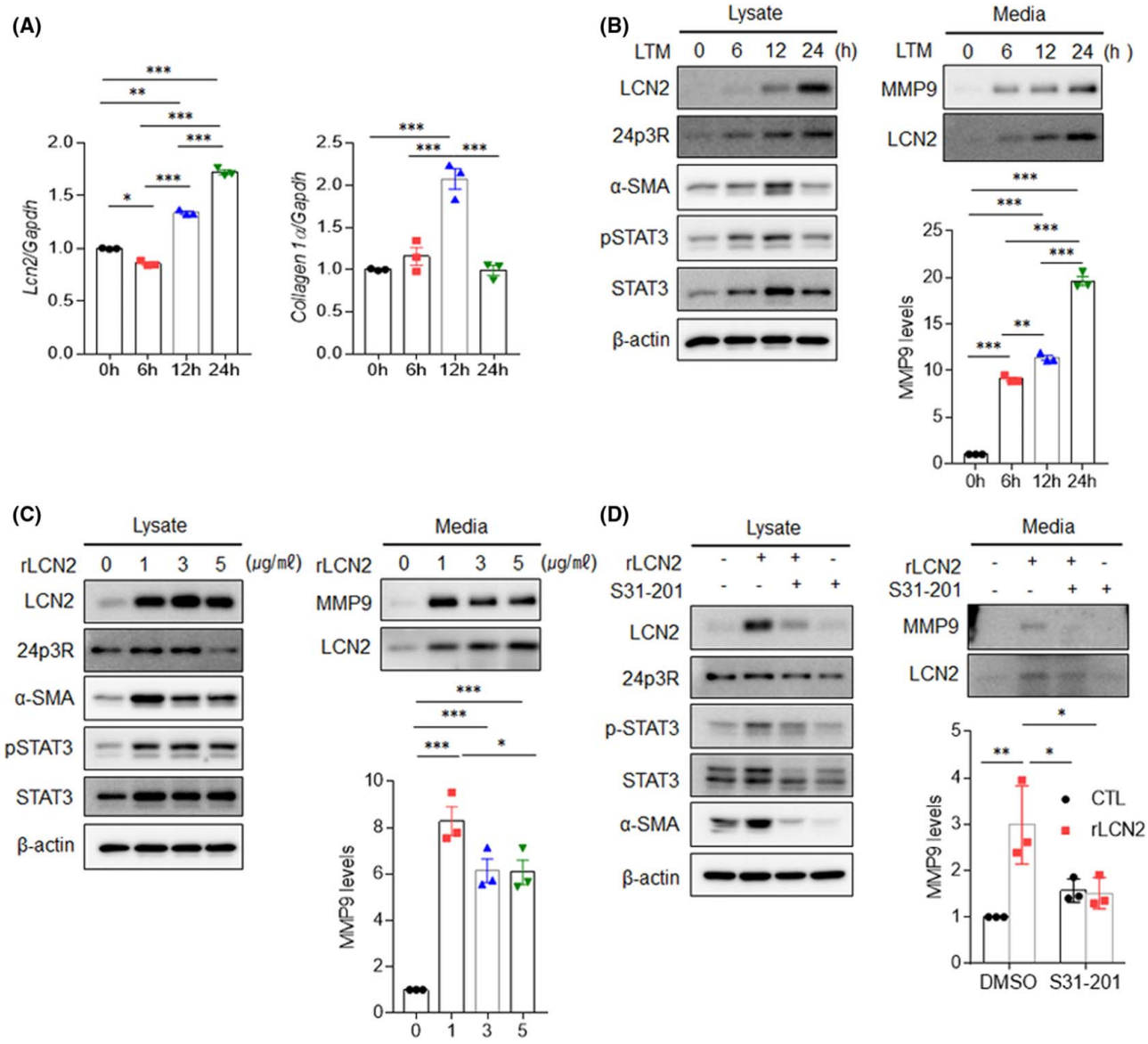


**FIGURE 7** Lipocalin-2 (LCN2) activates and induces secretion of matrix metalloproteinase 9 (MMP9) from isolated primary mouse hepatic stellate cells (mHSCs) from Ob/Ob mice. (A) Expression of messenger RNA *Lcn2* and *collagen 1α* in LPS-treated medium (LTM)-treated mHSCs was measured by real-time polymerase chain reaction ($n = 3$). (B) Western blot analysis of LCN2, 24p3R, α-smooth muscle actin (α-SMA), phosphorylated signal transducer and activator of transcription 3 (pSTAT3), and signal transducer and activator of transcription 3 (STAT3) in mHSCs after LTM treatment. Western blot analysis of MMP9 and LCN2 in the supernatant medium of mHSCs after LTM treatment. (C) Western blot analysis of LCN2, 24p3R, α-SMA, pSTAT3, and STAT3 in mHSCs after recombinant LCN2 (rLCN2) treatment. Western blot analysis of MMP9 and LCN2 in the supernatant medium of mHSCs after rLCN2 treatment. (D) Western blot analysis of LCN2, 24p3R, α-SMA, pSTAT3, and STAT3 in mHSCs after S31-201 treatment. Western blot analysis of MMP9 in the supernatant medium of mHSCs after S31-201 treatment ($n = 3$). For (A–C), significance was determined by one-way analysis of variance (ANOVA). For (D), significance was determined by two-way ANOVA. $^*p < 0.05$, $^{**}p < 0.01$, $^{***}p < 0.001$. CTL, control; DMSO, Dimethyl sulfoxide; Gapdh, glyceraldehyde 3-phosphate dehydrogenase.

## LCN2 promotes migration of LTM-activated HSCS via 24P3R

To assess the role of secreted LCN2 in the activation of mHSCs, we knocked down 24p3R in mHSCs using small interfering RNA (siRNA). Notably, we found decreased LCN2, α-SMA, and pSTAT3 in 24p3R-depleted mHSCs compared with scramble siRNA-transfected mHSCs (Figure 8A). The secretion of MMP9 and LCN2 protein by LTM-treated mHSCs was also inhibited by 24p3R siRNA transfection (Figure 8A). As expected, the decrease in Nile Red staining induced by LTM was significantly reversed by si24p3R knockdown in mHSCs (Figure 8B). As previously reported, when HSCs are activated, they proliferate, migrate to sites of liver injury, and secrete MMPs for ECM degradation.[29–31] As LTM and rLCN2 increased mHSC activation-induced MMP9 secretion,

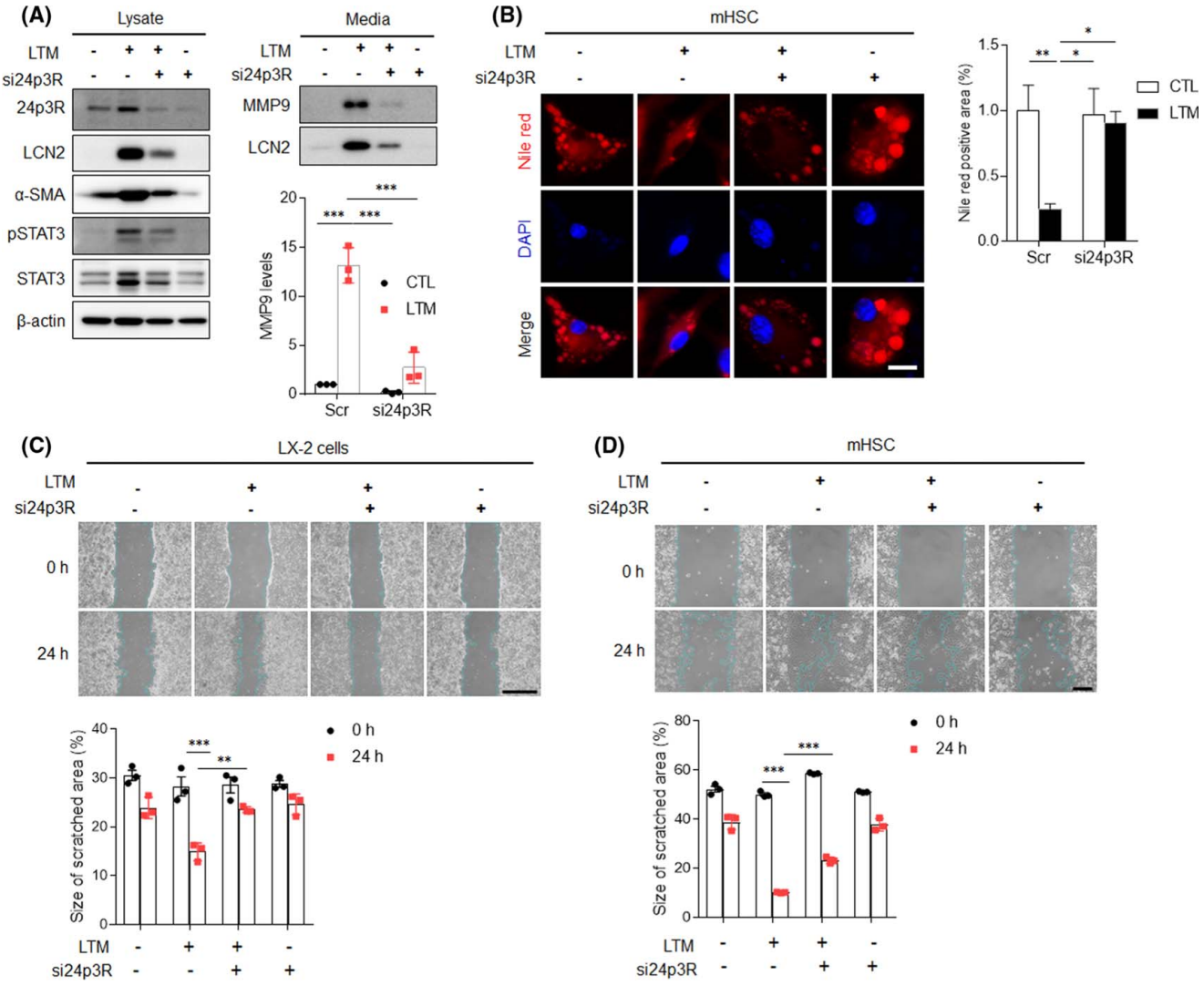


**FIGURE 8** Effects of 24p3R inhibition on activation and migration of primary mouse hepatic stellate cells (mHSCs). (A) Western blot analysis of 24p3R, lipocalin-2 (LCN2), α-smooth muscle actin (α-SMA), phosphorylated signal transducer and activator of transcription 3 (pSTAT3), and signal transducer and activator of transcription 3 (STAT3) in mHSCs from Ob/Ob mice after LPS-treated medium (LTM) and si24p3R treatment. Western blot analysis of matrix metalloproteinase 9 (MMP9) and LCN2 in the supernatant medium of mHSCs after LTM and si24p3R treatment. (B) Representative images of Nile Red staining of LTM-treated mHSCs with or without si24p3R and quantification of Nile Red–stained lipid droplets in mHSCs. Nuclei were counterstained with DAPI. Scale bar, 10 μm. (C,D) Wound healing migration assay was used to investigate the effect of 24p3R on the migration of (C) LX-2 cells and (D) mHSCs following 24 h of cotreatment with LTM and si24p3R ($n = 3$). Scale bar, (C) 500 μm, (D) 50 μm. Significance was determined by two-way analysis of variance. *$p < 0.05$, **$p < 0.01$, ***$p < 0.001$. CTL, control; DAPI, 4′, 6-diamidino-2-phenylindole; Scr, Scramble.

we assessed the effect of LCN2 on the migration of mHSCs using a wound healing assay. Twenty-four hours after LTM treatment, knockdown of 24p3R by siRNA inhibited LTM-induced migration of LX-2 cells and mHSCs (Figure 8C,D). In addition to the reduced levels of LCN2, α-SMA, and pSTAT3 observed in LCN2-depleted mHSCs, the secreted MMP9 and LCN2 proteins by LTM-treated mHSCs was also inhibited by LCN2 siRNA transfection (Figure S12). Collectively, these results demonstrate that secreted LCN2 may activate and promote the migration of HSCs through LCN2/24p3R under leptin-deficient conditions.

## DISCUSSION

In this study, we discovered that LCN2 is an HSC activator that is highly elevated in HFD-fed ob/ob mice with NASH. Mechanistically, LCN2 depletion in ob/ob mice attenuated NASH by downregulating MMP9/STAT3 signaling in HSCs. This study demonstrates that LCN2-mediated HSC activation increases α-SMA and MMP9 production by promoting STAT3 signaling. In particular, HFD feeding–induced HSC activation, which was characterized by reduced cytoplasmic LD accumulation, was inhibited by LCN2 depletion, 24p3R knockdown, or a STAT3 inhibitor. Therefore, our

findings suggest that LCN2 may drive the progression of liver steatosis to NASH with fibrosis through HSC activation.

Leptin was the first adipocytokine directly associated with hepatic fibrosis.[32] Although leptin promotes progression to NASH,[33] we observed that circulating leptin levels remained constant after 10 weeks of HFD feeding. $CCl_4$-treated mice showed massive hepatic fibrosis with F4/80-positive macrophage infiltration without elevated leptin protein or hepatic TG levels. Although ob/ob mice generally develop hepatic steatosis, this does not lead to NASH. However, an HFD, methionine- and choline-deficient diet, and low-dose LPS diet cause hepatic fibrosis in ob/ob mice.[9] Consistent with previous studies, we observed extensive hepatic fibrosis in ob/ob mice after 20 weeks of HFD feeding. Notably, LCN2 expression was positively associated with hepatic α-SMA protein level in HFD-fed ob/ob mice. LCN2 appears to play paradoxical roles in different targeting cells or liver injury models including NASH and liver fibrosis.[14,34,35] Xu et al. showed that hepatocyte-derived LCN2 protects against high-fat/cholesterol fructose diet–fed NAFLD.[14] However, consistent with the results of our study, Chen et al. found that LCN2 deletion attenuates liver fibrosis in a mouse model of alcoholic hepatitis and $CCl_4$-treated liver injury.[34] Thus, our findings indicate that LCN2 may promote HFD-induced liver fibrosis without leptin production.

To explore the mechanism of leptin-independent NASH, we performed RNA-sequencing analysis to verify DEGs related to LCN2-related inflammation and fibrosis in the liver of WT and ob/ob mice fed an ND or HFD. Our findings are consistent with those of previous studies showing that LCN2 is associated with ECM formation and migration of activated HSCs.[36–38] MMPs degrade hepatic ECM proteins in chronic liver injury models.[39] Within the MMP family, MMP9 is secreted and activated by HSCs during their transdifferentiation process.[40] Multiple studies show evidence of increased hepatic MMP9 protein levels in experimental cirrhosis.[41,42] In particular, MMP9 binds LCN2 and forms a MMP9/LCN2 complex, preventing the degradation of MMP9.[43] Thus, we hypothesized that elevated LCN2 promotes MMP9-mediated ECM degradation and NASH progression. As expected, hepatic MMP9 activity as revealed by zymography was correlated with hepatic expression of MMP9 protein in HFD-fed ob/ob mice. Duolink assay also showed an increase in LCN2/MMP9-positive cells in the liver of HFD-fed ob/ob mice. Our findings, on the other hand, suggest that CR-induced weight reduction may decrease LCN2 production, thereby reducing HSC activation and hepatic MMP9/p-STAT3 expressions. Furthermore, LCN2 depletion reduced hepatic MMP9 protein levels in DKO mice, whereas rLCN2 increased MMP9 protein levels in the liver of ob/ob mice. In addition, secreted LCN2-containing medium induced MMP9 and LCN2 production in LX-2 cells and mHSCs. Previous studies show that the transcription factor STAT3 directly regulates *Lcn2* and *Mmp9* gene expression.[18,19] In this study, a STAT3 phosphorylation inhibitor downregulated α-SMA and MMP9 levels in LCN2/24p3R-activated HSCs. In line with our finding that 24p3R inhibition reduced α-SMA expression in LTM-treated mHSCs, 24p3R silencing was previously found to abolish *α-SMA* mRNA in cortical collection ducts.[44] A recent study indicates that LCN2-activated 24p3R is a critical mediator exclusively produced in the liver during NASH progression.[45] Taken together, these findings indicate that HSC activation-induced α-SMA and MMP9 production may play an important role in leptin-independent hepatic fibrosis through LCN2/24p3R/STAT3-mediated signaling.

Because HSCs promote ECM degradation and hepatic inflammation in chronic liver disease, antifibrotic therapy aims to prevent HSC activation, proliferation, or migration in liver fibrosis.[46] Other studies suggest that LCN2 is an aggravating factor of NASH due to its interaction with immune cells.[13,47] However, in this study, LCN2-positive cells were observed not only in Ly6G- and MPO-positive neutrophils and CD68-positive macrophages but also in α-SMA–positive HSCs. These results strongly support the existence of a mechanism by which increased LCN2 activates HSCs in addition to immune cell infiltration. Moreover, in our in vitro experiments, we confirmed that LCN2 receptor binding promotes the migration of activated HSCs via MMP9 secretion. Taken together, our findings suggest that LCN2 acts as a fibrotic agent that regulates the activation and migration of HSCs in HFD-fed ob/ob mice.

A previous study reports that LCN2 may function in an autocrine or paracrine manner by interacting with 24p3R in the hippocampus of diabetic mice.[48] Another study shows that neutrophils and macrophages express 24p3R, which regulates LCN2 secretion and expression in chronic peripheral inflammation.[49] Thus, although STAT3 is known to directly regulate LCN2 gene expression,[18,19] the autocrine or paracrine mechanisms of action of LCN2 have yet to be determined. In the present study, we found that pSTAT3 was increased by LTM or rLCN2 treatment in mHSCs and was inhibited by S31-101. Furthermore, we confirmed that 24p3R was increased in LTM-treated mHSCs in a time-dependent manner. Thus, we suggest that LCN2 could increase its own expression in activated HSCs through binding 24p3R.

On the other hand, levels of perilipin 2 increase during NAFLD development, and perilipin 2 overexpression promotes the uptake of lipids into LDs in humans and mice.[50,51] By contrast, perilipin 2 knockout mice are resistant to obesity-induced NAFLD.[52] Notably, we found that hepatic perilipin 2 was significantly

reduced, along with lipogenic proteins such as ACC1, SCD1, and FAS, in HFD-fed ob/ob mice compared with ND-fed ob/ob mice. These results are consistent with evidence that two prominent features of HSC activation in liver fibrosis are a loss of cytoplasmic LDs around portal triads and an increase in α-SMA. In line with reduced liver steatosis, perilipin 2–deficient mice or perilipin 2 antisense oligonucleotide–treated mice show attenuated HFD-induced NAFLD.[53,54] Conversely, although perilipin 2 and lipogenic proteins were reduced in HFD-fed ob/ob mice, LCN2-mediated HSC activation may promote NASH progression, which may explain why perilipin 2 was decreased and α-SMA was increased in mHSCs from HFD-fed ob/ob mice. Based on our findings, we suggest that, although lipid uptake may be increased in hepatocytes, the loss of LDs during HSC activation may play an important role in hepatic fibrosis and could be mediated by LCN2.

In conclusion, we demonstrate that LCN2, which increases immune cell infiltration in the liver via chemokines, or its receptor also activates HSCs. Although we do not fully understand the causes of increased LCN2, we provide evidence that LCN2 promotes the activation and migration of HSCs and is a causative agent of liver fibrosis in HFD-fed ob/ob mice. Therefore, LCN2 could serve as an antifibrotic target for protecting against obesity-induced hepatic fibrosis progression.

## ACKNOWLEDGMENT

We thank Jaemin Yoo for technical support and Woori Kwak and C&K Genomics for RNA sequencing analysis.

## AUTHOR CONTRIBUTIONS

Kyung Eun Kim and Jaewoong Lee conceived and performed most experiments, analyzed the data, and prepared the manuscript; Gu Seob Roh conceived and designed the study, supervised the project, analyzed the data, and wrote the manuscript; Hyun Joo Shin, Eun Ae Jeong, Hye Min Jang, Yu Jeong Ahn, Hyeong Seok An, and Jong Youl Lee helped to perform experiments; Meong Cheol Shin performed recombinant LCN2 and leptin purification; Won Ho Kim and Soo Kyoung Kim were involved in scientific discussions of the manuscript; and Won Gi Yoo performed RNA sequencing–based transcriptome analysis (RNA-seq data from this study are deposited under the NCBI Project Accession Number: GSE167264).

## FUNDING INFORMATION

This study was supported by the Basic Science Research Program through the National Research Foundation of Korea (No. 2015R1A5A2008833, 2018R1A6A3A01012427, and 2021R1A2C2093913)

## CONFLICT OF INTEREST

Nothing to report.

## REFERENCES

1. Byrne CD, Targher G. NAFLD: a multisystem disease. J Hepatol. 2015;62:S47–64.
2. Friedman SL, Neuschwander-Tetri BA, Rinella M, Sanyal AJ. Mechanisms of NAFLD development and therapeutic strategies. Nat Med. 2018;24:908–22.
3. Chalasani N, Younossi Z, Lavine JE, Charlton M, Cusi K, Rinella M, et al. The diagnosis and management of non-alcoholic fatty liver disease: practice guidance from the American Association for the Study of Liver Diseases. Hepatology. 2018;67:328–57.
4. Boutari C, Perakakis N, Mantzoros CS. Association of adipokines with development and progression of nonalcoholic fatty liver disease. Endocrinol Metab (Seoul). 2018;33:33–43.
5. Tsuchida T, Friedman SL. Mechanisms of hepatic stellate cell activation. Nat Rev Gastroenterol Hepatol. 2017;14:397–411.
6. Schwabe RF, Tabas I, Pajvani UB. Mechanisms of fibrosis development in nonalcoholic steatohepatitis. Gastroenterology. 2020;158:1913–28.
7. Zisser A, Ipsen DH, Tveden-Nyborg P. Hepatic stellate cell activation and inactivation in NASH-fibrosis-roles as putative treatment targets? Biomedicine. 2021;9:365.
8. Takahashi Y, Soejima Y, Fukusato T. Animal models of nonalcoholic fatty liver disease/nonalcoholic steatohepatitis. World J Gastroenterol. 2012;18:2300–8.
9. Kristiansen MNB, Veidal SS, Rigbolt KTG, Tølbøl KS, Roth JD, Jelsing J, et al. Obese diet-induced mouse models of non-alcoholic steatohepatitis-tracking disease by liver biopsy. World J Hepatol. 2016;8:673–84.
10. Kjeldsen L, Johnsen AH, Sengeløv H, Borregaard N. Isolation and primary structure of NGAL, a novel protein associated with human neutrophil gelatinase. J Biol Chem. 1993;268:10425–32.
11. Asimakopoulou A, Weiskirchen S, Weiskirchen R. Lipocalin 2 (LCN2) expression in hepatic malfunction and therapy. Front Physiol. 2016;7:430.
12. Moschen AR, Adolph TE, Gerner RR, Wieser V, Tilg H. Lipocalin-2: a master mediator of intestinal and metabolic inflammation. Trends Endocrinol Metab. 2017;28:388–97.
13. Ye D, Yang K, Zang S, Lin Z, Chau HT, Wang Y, et al. Lipocalin-2 mediates non-alcoholic steatohepatitis by promoting neutrophil-macrophage crosstalk via the induction of CXCR2. J Hepatol. 2016;65:988–7.
14. Xu Y, Zhu Y, Jadhav K, Li Y, Sun H, Yin L, et al. Lipocalin-2 protects against diet-induced nonalcoholic fatty liver disease by targeting hepatocytes. Hepatol Commun. 2019;3:763–5.
15. Zhang HP, Chen MY, Xu YX, Xu GY, Chen JR, Wang YM, et al. An effective live attenuated vaccine against Aeromonas veronii infection in the loach (Misgurnus anguillicaudatus). Fish Shellfish Immunol. 2020;104:269–78.
16. Ardi VC, Kupriyanova TA, Deryugina EI, Quigley JP. Human neutrophils uniquely release TIMP-free MMP-9 to provide a potent catalytic stimulator of angiogenesis. Proc Natl Acad Sci U S A. 2007;104:20262–7.
17. Koh SA, Lee KH. HGF mediated upregulation of lipocalin 2 regulates MMP9 through nuclear factor-κB activation. Oncol Rep. 2015;34:2179–87.
18. Xiang Y, Li JP, Guo W, Wang DQ, Yao A, Zhang HM, et al. Novel interactions between ERα-36 and STAT3 mediate breast cancer cell migration. Cell Commun Signal. 2019;17:93.
19. Xu MJ, Feng D, Wu H, Wang H, Chan Y, Kolls J, et al. Liver is the major source of elevated serum lipocalin-2 levels after bacterial infection or partial hepatectomy: a critical role for IL-6/STAT3. Hepatology. 2015;61:692–702.
20. Jeon BT, Heo RW, Jeong EA, Yi CO, Lee JY, Kim KE, et al. Effects of caloric restriction on O-GlcNAcylation, ca(2+) signaling, and learning impairment in the hippocampus of Ob/Ob mice. Neurobiol Aging. 2016;44:127–37.

21. Duarte S, Baber J, Fujii T, Coito AJ. Matrix metalloproteinases in liver injury, repair and fibrosis. Matrix Biol. 2015; 44–46:147–56.
22. Vallabhapurapu S, Karin M. Regulation and function of NF-κB transcription factors in the immune system. Annu Rev Immunol. 2009;27:693–733.
23. Iwakiri Y. Nitric oxide in liver fibrosis: the role of inducible nitric oxide synthase. Clin Mol Hepatol. 2015;21:319–25.
24. Aram G, Potter JJ, Liu X, Torbenson MS, Mezey E. Lack of inducible nitric oxide synthase leads to increased hepatic apoptosis and decreased fibrosis in mice after chronic carbon tetrachloride administration. Hepatology. 2008;47:2051–8.
25. Blaner WS, O'Byrne SM, Wongsiriroj N, Kluwe J, D'Ambrosio DM, Jiang H, et al. Hepatic stellate cell lipid droplets: a specialized lipid droplet for retinoid storage. Biochim Biophys Acta. 2009;1791:467–73.
26. Lee TF, Mak KM, Rackovsky O, Lin YL, Kwong AJ, Loke JC, et al. Downregulation of hepatic stellate cell activation by retinol and palmitate mediated by adipose differentiation-related protein (ADRP). J Cell Physiol. 2010;223:648–57.
27. Trivedi P, Wang S, Friedman SL. The power of plasticity-metabolic regulation of hepatic stellate cells. Cell Metab. 2021; 33:242–57.
28. Libby AE, Bales ES, Monks J, Orlicky DJ, McManaman JL. Perilipin-2 deletion promotes carbohydrate-mediated browning of white adipose tissue at ambient temperature. J Lipid Res. 2018; 59:1482–500.
29. Ramezani-Moghadam M, Wang J, Ho V, Iseli TJ, Alzahrani B, Xu A, et al. Adiponectin reduces hepatic stellate cell migration by promoting tissue inhibitor of metalloproteinase-1 (TIMP-1) secretion. J Biol Chem. 2015;290:5533–42.
30. Lotersztajn S, Julien B, Teixeira-Clerc F, Grenard P, Mallat A. Hepatic fibrosis: molecular mechanisms and drug targets. Annu Rev Pharmacol Toxicol. 2005;45:605–28.
31. Friedman SL. Mechanisms of hepatic fibrogenesis. Gastroenterology. 2008;134:1655–69.
32. Saxena NK, Anania FA. Adipocytokines and hepatic fibrosis. Trends Endocrinol Metab. 2015;26:153–61.
33. Imajo K, Fujita K, Yoneda M, Nozaki Y, Ogawa Y, Shinohara Y, et al. Hyperresponsivity to low-dose endotoxin during progression to nonalcoholic steatohepatitis is regulated by leptin-mediated signaling. Cell Metab. 2012;16:44–54.
34. Chen J, Argemi J, Odena G, Xu MJ, Cai Y, Massey V, et al. Hepatic lipocalin 2 promotes liver fibrosis and portal hypertension. Sci Rep. 2020;10:15558.
35. Asimakopoulou A, Borkham-Kamphorst E, Henning M, Yagmur E, Gassler N, Liedtke C, et al. Lipocalin-2 (LCN2) regulates PLIN5 expression and intracellular lipid droplet formation in the liver. Biochim Biophys Acta. 2014;1842:1513–24.
36. Wang Q, Liu X, Zhang J, Lu L, Feng M, Wang J. Dynamic features of liver fibrogenesis and fibrosis resolution in the absence of matrix metalloproteinase9. Mol Med Rep. 2019;20: 5239–48.
37. Tarrats N, Moles A, Morales A, Garcia-Ruiz C, Fernandez-Checa JC, Mari M. Critical role of tumor necrosis factor receptor 1, but not 2, in hepatic stellate cell proliferation, extracellular matrix remodeling, and liver fibrogenesis. Hepatology. 2011;54:319–27.
38. Wang Z, Li J, Xiao W, Long J, Zhang H. The STAT3 inhibitor S3I-201 suppresses fibrogenesis and angiogenesis in liver fibrosis. Lab Invest. 2018;98:1600–3.
39. Benyon RC, Arthur MJ. Extracellular matrix degradation and the role of hepatic stellate cells. Semin Liver Dis. 2001;21:373–84.
40. Han YP, Yan C, Zhou L, Qin L, Tsukamoto H. A matrix metalloproteinase-9 activation cascade by hepatic stellate cells in trans-differentiation in the three-dimensional extracellular matrix. J Biol Chem. 2007;282:12928–39.
41. Kossakowska AE, Edwards DR, Lee SS, Urbanski LS, Stabbler AL, Zhang CL, et al. Altered balance between matrix metalloproteinases and their inhibitors in experimental biliary fibrosis. Am J Pathol. 1998;153:1895–902.
42. Kim JW, Lee SH, Jeong SH, Kim H, Ahn KS, Cho JY, et al. Increased urinary lipocalin-2 reflects matrix metalloproteinase-9 activity in chronic hepatitis C with hepatic fibrosis. Tohoku J Exp Med. 2010;222:319–27.
43. Yan L, Borregaard N, Kjeldsen L, Moses MA. The high molecular weight urinary matrix metalloproteinase (MMP) activity is a complex of gelatinase B/MMP-9 and neutrophil gelatinase-associated lipocalin (NGAL). Modulation of MMP-9 activity by NGAL. J Biol Chem. 2001;276:37258–65.
44. Dizin E, Hasler U, Nlandu-Khodo S, Fila M, Roth I, Ernandez T, et al. Albuminuria induces a proinflammatory and profibrotic response in cortical collecting ducts via the 24p3 receptor. Am J Physiol Renal Physiol. 2013;305:F1053–63.
45. Mondal A, Bose D, Saha P, Sarkar S, Seth R, Kimono D, et al. Lipocalin 2 induces neuroinflammation and blood-brain barrier dysfunction through liver-brain axis in murine model of non-alcoholic steatohepatitis. J Neuroinflammation. 2020;17:201.
46. Wu J, Zern MA. Hepatic stellate cells: a target for the treatment of liver fibrosis. J Gastroenterol. 2000;35:665–72.
47. Li H, Feng D, Cai Y, Liu Y, Xu M, Xiang X, et al. Hepatocytes and neutrophils cooperatively suppress bacterial infection by differentially regulating lipocalin-2 and neutrophil extracellular traps. Hepatology. 2018;68:1604–20.
48. Bhusal A, Rahman MH, Lee IK, Suk K. Role of hippocampal Lipocalin-2 in experimental diabetic encephalopathy. Front Endocrinol (Lausanne). 2019;10:25.
49. Jha MK, Jeon S, Jin M, Ock J, Kim JH, Lee WH, et al. The pivotal role played by lipocalin-2 in chronic inflammatory pain. Exp Neurol. 2014;254:41–53.
50. Motomura W, Inoue M, Ohtake T, Takahashi N, Nagamine M, et al. Up-regulation of ADRP in fatty liver in human and liver steatosis in mice fed with high fat diet. Biochem Biophys Res Commun. 2006;340:1111–8.
51. Gao J, Serrero G. Adipose differentiation related protein (ADRP) expressed in transfected COS-7 cells selectively stimulates long chain fatty acid uptake. J Biol Chem. 1999;274:16825–30.
52. McManaman JL, Bales ES, Orlicky DJ, Jackman M, MacLean PS, Cain S, et al. Perilipin-2-null mice are protected against diet-induced obesity, adipose inflammation, and fatty liver disease. J Lipid Res. 2013;54:1346–59.
53. Chang BH, Li L, Paul A, Taniguchi S, Nannegari V, Heird WC, et al. Protection against fatty liver but normal adipogenesis in mice lacking adipose differentiation-related protein. Mol Cell Biol. 2006;26:1063–76.
54. Imai Y, Varela GM, Jackson MB, Graham MJ, Crooke RM, Ahima RS. Reduction of hepatosteatosis and lipid levels by an adipose differentiation-related protein antisense oligonucleotide. Gastroenterology. 2007;132:1947–54.


**How to cite this article:** Kim KE, Lee J, Shin HJ, Jeong EA, Jang HM, Ahn YJ, et al. Lipocalin-2 activates hepatic stellate cells and promotes nonalcoholic steatohepatitis in high-fat diet–fed Ob/Ob mice. Hepatology. 2023;77:888–901. https://doi.org/10.1002/hep.32569